Vectorcardiographic and electrocardiographic analysis for identification of patients with myocardial infarction

Raúl Correa[1,*], Pedro David Arini[2, 3 §], Lorena Correa[1 §],
Max Valentinuzzi[3 §] and Eric Laciar[1 §]

[1]Gabinete de Tecnología Médica, Facultad de Ingeniería, Universidad Nacional de San Juan (UNSJ), San Juan, Argentina, rcorrea@gateme.unsj.edu.ar; lcorrea@gateme.unsj.edu.ar; laciar@gateme.unsj.edu.ar

[2]Instituto Argentino de Matemática (IAM) "Alberto P. Calderón", Consejo Nacional de Investigaciones Científicas y Técnicas (CONICET), Buenos Aires, Argentina, pedro.arini@conicet.gov.ar

[3]Instituto de Ingeniería Biomédica (IIBM), Facultad de Ingeniería (FI), Universidad de Buenos Aires (UBA), Buenos Aires, Argentina, maxvalentinuzzi@arnet.com.ar

[§] These authors contributed equally to this work and the corresponding author (*) takes responsibility for all aspects of the reliability and freedom from bias of the data presented and their discussed interpretation

Abstract

Background

The largest morbidity and mortality group worldwide continues to be that suffering Myocardial Infarction (MI). The use of vectorcardiography (VCG) and electrocardiography (ECG) has improved the diagnosis and characterization of this cardiac condition.

Objective

Herein, we applied a novel ECG-VCG combination technique to identifying 95 patients with MI and to differentiating them from 52 healthy reference subjects. Subsequently, and with a similar method, the location of the infarcted area permitted patient classification.

Methods

We analyzed 5 depolarization and 4 repolarization indexes, say: (a) volume; (b) planar area; (c) QRS loop perimeter; (d) QRS vector difference; (e-g) Area under the QRS complex, ST segment and T-wave in the (X, Y, Z) leads; (f) ST-T Vector Magnitude Difference; (h) T-wave Vector Magnitude Difference; and (i) the spatial angle between the QRS complex and the T-wave.

For classification, patients were divided into two groups according to the infarcted area, that is, anterior or inferior sectors (MI-ant and MI-inf, respectively).

Results

Our results indicate that several ECG and VCG parameters show significant differences (p-value<0.05) between Healthy and MI subjects, and between MI-ant and MI-inf. Moreover, combining five parameters, it was possible to classify the MI and healthy subjects with a sensitivity = 95.8%, a specificity = 94.2%, and an accuracy = 95.2%, after applying a linear discriminant classifier method. Similarly, combining eight indexes, we could separate out the MI patients in MI-ant vs MI-inf with a sensitivity = 89.8%, 84.8%, respectively, and an accuracy = 89.8%.

Conclusions

The new multivariable MI patient identification and localization technique, based, on ECG and VCG combination indexes, offered excellent performance to differentiating populations with MI from healthy subjects. Furthermore, this technique might be applicable to estimating the infarcted area localization. In addition, the proposed method would be an alternative diagnostic technique in the emergency room.

Keywords:

Myocardial Infarction, Electrocardiography, Vectorcardiography, Discriminant Analysis

1-INTRODUCTION

Myocardial Infarction (MI) has been long recognized as the main cause of death worldwide (1). In addition, cardiac ischemia (CI) causes changes in the energy dependent (ATP) pumps located within the cardiac cells sarcolemma, which modifies the transmembrane potential, usually recorded as morphological changes in the ECG and VCG. Moreover, a sudden occlusion in one of the major coronary arteries (in the absence of a coronary collateral flow) results in transmural ischemia, the first step of the so-called ischemic cascade phenomenon. The chain of events usually proceeds in a sequence, that is: 1) ischemia; 2) diastolic dysfunction (poor relaxation); 3) systolic dysfunction (weak contraction); 4) angina pectoris (brought about by accumulation of metabolites); 5) infarction and eventual necrosis (1).

Within the vectorcardiography framework, the momentary cardiac electrical activity is representable by a single vector in the Euclidian space, i.e., the heart vector, and the VCG precisely describes both components, magnitude and direction, as time proceeds.

Different studies (1) have demonstrated that ischemia modifies ECG segments and waves of left ventricular depolarization and repolarization (QRS-complex and ST-T segment). Similarly, other researchers have verified that the QRS-complex and the T-wave loops of the VCG also undergo modifications due to total coronary or partial obstructions. Manocha and Singh (2) summarized most of ECG techniques to CI detection and concluded that the sensitivity and positive predictability of the ST-segment lead to an average value of 87–89% and 90–92%, respectively. Dilger *et. al* proposed the use of predictive variables from previous history, ECG, and clinical chemical parameters in order to minimize the initial diagnostic uncertainty of MI (3). We have recently proposed three studies that use the combination of some new parameters computed from original VCGs, with the alternative vectorcardiographic parameters to CI monitoring and detection. In (4), we studied a set of QRS-loop parameters and ST_{VM} computed from resting records in order to distinguish ischemic patients with diagnosed Coronary Acute Disease from healthy subjects. We concluded that QRS loop parameters combined with ST_{VM} improved the sensitivity and specificity values with respect to those obtained using only the ST_{VM} index. Furthermore, in (5), we extended the use of a similar set of

QRS loop parameters to myocardial ischemia monitoring. It was demonstrated that these parameters, combined with the classic indexes, increase sensitivity and specificity for acute ischemia monitoring. Finally, in (6), we proposed a vectorcardiographic analysis of the ventricular repolarization (ST-T interval) to monitor acute myocardial ischemia. To this end, we computed four vectorcardiographic parameters and two conventional indexes before and during Coronary Angioplasty. As conclusion: The sensitivity and specificity for acute ischemia monitoring increased with the use of only two vectorcardiographic parameters.

Several researchers have proposed different techniques to identifying patients with MI, based on the ECG, among which we can mention, Bakul *et al.*(7), who have developed a set of features called *Relative Frequency Band Coefficient* for automatic identification of MI risk. Moreover, Keshtkar *et al.* (8) proposed the evaluation of the *wavelet coefficients set* computed on the *average ECG signal* through neural networks as indices to detect MI. Furthermore, Muhammad *et al.* (9) presented automatic detection and localization of MI using k-Nearest Neighbor (KNN) classifier and Time Domain features of each beat in the ECG signal, such as T-wave amplitude. In a recent work, Safdarian *et al.* (10) proposed two new features, i.e., T-wave integral and total integral as extracted features from one ECG cycle for the infarcted area detection and localization.

In this paper, we evaluated a novel technique for processing ECG and VCG signals in order to identify patients with MI and to differentiate them from healthy subjects. Furthermore, the technique performance was evaluated in two different heart areas. The objective of this study is to determine near its outset, and as accurately as possible, when a patient has suffered MI, and also to predict its location. Advantages of the proposed combined ECG and VCG technique are it is non-invasive, and it does not lead to any adverse effect if applied repeatedly.

2-MATERIALS

We used 161 ECG records from 95 patients with MI (71 men, age 58 ± 10 yrs, and 24 women, age 64 ± 12 yrs) that were obtained after the MI episode (denoted as MI-patients). Although the *Physikalisch-Technische Bundesanstalt* (PTB) (11) database contains from 1 to 7

ECG's per patient, this study only used those obtained within the first week after MI. The areas of myocardial necrosis were anterior (n=14), antero-lateral (n=10), antero-septal (n=24), antero-septo-lateral (n=1), inferior (n=23), infero-lateral (n=17), and infero-postero-lateral (n=6). Since the number of patients for each infarcted area is small, we grouped them into two sets, a) patients that have the anterior area affected (n=49), denoted as MI-Anterior, and b) those who have infarcted the inferior zone (n=46), denoted as MI-Inferior.

It is important to highlight that, of the 290 subjects contained in the PTB database, only 148 had suffered MI, 126 of these include in the header file the MI localization, and just 95 of these include at least one ECG recording obtained during the week after infarction and the affected area, say, the inferior or the anterior heart region.

ECG's from 52 healthy subjects (39 men, age 42 ± 14 yrs, and 13 women, age 48 ± 19yrs) were also used as a control group (denoted as healthy subject). All data were obtained from the PTB database of the National Metrology Institute of Germany, available at *Physionet*. Each record includes 15 simultaneous signals: The conventional 12-leads (I, II, III, aVR, aVL, aVF, V1-V6) together with the 3-Frank X, Y, Z system. Each was digitized at 1000 Hz, with 16 bits of amplitude resolution (11). It is underlined that only the orthogonal ECG leads (X, Y, Z) were used to derive the VCG (4). The data have been studied anonymously, using publicly available secondary data; therefore no ethics statement is required for this investigation (12). All study subjects were listed in 2 supplementary Tables.

3-METHODS

In order to reduce low and high frequency noise, all ECG records were pre-processed with a band-pass filter (Butterworth, 4^{th} order, 0.2-100 Hz, bidirectional). Moreover, a notch filter (Butterworth, 2^{th} order, 50/60 Hz, bidirectional) minimized power-line interference. Besides, a cubic spline interpolation filter allowed attenuation of the ECG baseline drifts and respiratory artifacts. Thereafter, the QRS complexes and their corresponding initial and final endpoints were detected in each ECG record, that is:

a) QRS complex detection: In this phase, each ECG record is first decomposed with the Continuous Wavelet Transform (CWT) and a prototype “Haar”. Then, each QRS complex is detected using an algorithm based on a threshold applied to the time-scale representation obtained with CWT (13)

b) ECG delineation: In this stage, each ECG record is decomposed using the Discrete Wavelet Transform (DWT), prototype quadratic splines, achieving d1, d2, d3 and d4 detail signals (14). Thereafter, the T-wave maximum amplitude (T-wave peak) and their endpoints can be determined on the basis of the QRS detected complexes and the relation between the characteristic points of the ECG and the maximum and minimum module pairs. On the beat where the T-wave endpoints were not correctly detected, they were set 80 ms before and 120 ms after the T-wave peak.

Excessively noisy beats (with a RMS noise level > 40μV, measured within a 40 ms window located at 2/3 of the RR interval) were excluded. Additionally, ectopic beats were also eliminated by comparing incoming signals against a previously established template by means of a cross-correlation technique. A visually low-noise normal beat extracted from the ECG record was selected as template (or reference) beat, as proposed in (15).

In this, way we have processed about 132 ± 24 and 158± 32 beat per ECG record for healthy and MI subjects, respectively. The excluded heartbeats average per ECG record was 3.5 ± 1 and 5.1 ± 6 for healthy and MI subjects, respectively

After such pre-processing, we carried out the feature extraction step. Figure 1 shows a general block diagram of the procedure.

figure 1

3.1- VCG – ECG’s features extraction

VCG is obtaining by drawing simultaneously in a 3-D plot the instantaneous amplitudes of XYZ orthogonal leads for each time sample in the temporal interval corresponding to the QRS complex. Herein, we analyzed 4 VCG parameters, 3 assessed on the QRS-loop and 1 between the QRS and T-loops. Also, 6 from the orthogonal ECG leads (X, Y, Z), 2 evaluated on

the QRS complex waves and 4 on the ST-T segment. In the same way as in a previous works, we have analyzed beat-to-beat morphological changes of the VCG and ECG (5,6).

We defined,

- *QRS-loop Volume* (***QRS***$_{V}$) [mV^3]: It is the set of points generated by the Minimal Convex Volume (MCV) enclosing all points of the QRS-loop. It aims at quantifying the loop flatness and morphology in 3D (5).

- *QRS-loop Planar Area* (***QRS***$_{PA}$) [mV^2]: It estimates the inner loop area, obtained by projecting the QRS-loop on the best-adjusted plane computed by least mean squares (Optimum Plane). It reflects hemodynamically-related cardiac pathologies (5) (Figure 2-a).

- *QRS-loop Perimeter* (***QRS***$_{P}$) [mV]: Computed around the QRS-loop projected over the Optimum Plane. It measures the loop total length and can detect loop contour changes (5).

- *Angle between the depolarization maximum vector (or QRS-complex waves) and the Repolarization (T-wave) in frontal, sagittal and transversal planes* (***aQRS-T***$_{F}$, ***a QRS-T***$_{S}$, ***aQRS-T***$_{T}$): It reflects the angular difference between the maximum QRS and T vectors and estimates the Ventricular Gradient. This parameter is a strong and independent predictor of cardiac mortality (16,17) (Figure 2-b).

- *Area under the QRS complex in X, Y and Z leads* (***aQRS***$_{X}$, ***aQRS***$_{Y}$, ***aQRS***$_{Z}$) [mVs]: It is defined as the difference area between the ECG signal at the current QRS complex and the abscissa. It estimates depolarization energy (Figure 2-c).

- *QRS-Vector Difference* (***QRS***$_{VD}$) [mVs]: It was defined (18) as the difference of the current QRS-complex area and the averaged QRS-complex area evaluated at the first 30s of each ECG record (Figure 2-d), i.e.

$$\boldsymbol{QRS}_{\mathrm{VD}} = \sqrt{A_X^2 + A_Y^2 + A_Z^2} \tag{1}$$

- *Area under the T-wave in X, Y and Z leads* (***aT***$_{X}$, ***aT***$_{Y}$, ***aT***$_{Z}$) [mVs]: It is defined as the difference area between the ECG signal at the current T-wave and the abscissa. It estimates repolarization energy (Figure 2-e).

- *T-wave Vector Difference* ($\boldsymbol{T}_{\mathrm{VD}}$) [mVs]: It is defined as the difference area between the ECG signal at the current T-wave interval and the reference T-wave interval, evaluated during the first 30s of each record (6) (Figure 2-f), that is,

$$\boldsymbol{T}_{\mathrm{VD}} = \left(dT_X^2 + dT_Y^2 + dT_Z^2\right)^{1/2} \tag{2}$$

The parameter estimates changes produced during middle and end ventricular repolarization.

- *Area under ST segment in X, Y and Z leads* ($\boldsymbol{aST}_{\mathrm{X}}$, $\boldsymbol{aST}_{\mathrm{Y}}$, $\boldsymbol{aST}_{\mathrm{Z}}$) [mVs]: It is defined as the difference area between the ECG signal at the current ST-segment and the abscissa. It estimates repolarization energy (Figure 2-g).

- *ST-T Vector Difference* ($\boldsymbol{ST}$-$\boldsymbol{T}_{\mathrm{VD}}$) [mVs]: It is defined as the difference in area between the ST-T interval (from the J-point to the T-wave end) and the reference ECG (at ST-T) evaluated at the first 30 s of each record (Figure 2-h), that is,

$$\boldsymbol{ST}\text{ - }\boldsymbol{T}_{\mathrm{VD}} = \left(dA_X^2 + dA_Y^2 + dA_Z^2\right)^{1/2} \tag{3}$$

Its objective is to estimate all changes produced during left ventricular repolarization (6).

figure 2

3. 2- Statistical analysis and features selection

All proposed parameters were computed for each detected sinus beat using the ECG (XYZ) and VCG records. Thereafter, the mean value of each parameter along the entire record was computed (that is, the mean value of the indexes computed in each beat). We analyzed the normality of these values using the D'Agostino-Pearson test in order to quantify the discrepancy between the parameters' distribution and the Gaussian distribution, since there are observations stating that the underlying Distribution of Variables is non-Gaussian. The statistical comparison between each parameter for healthy and MI patients was made by means of the non-parametric Mann-Whitney test.

The feature selection was performed with the Wilks Lambda (WL) stepwise method for identifying the variables that improve classification and reduce the number of variables in the

Linear Discriminant Analysis (LDA) (19). The WL measures the ratio between the intra-group dispersion and the general dispersion without distinction of groups (extra-group dispersion). If the WL value is small, close to 0, the total variability will be due to differences between groups and, thereby, variables with a lower WL value have a greater discriminating power (between groups) (20). Hence, the stepwise WL method consists of selecting a variable at each step, which, once incorporated to the discriminant function, produces the lowest WL value for the set of variables within the function.

Briefly, we selected five ECG-VCG features that produced the lowest WL for the classification between Healthy and MI subjects and denoted them as Best Combination (BC-H-MI). Similarly, we found 8 ECG-VCG features for the classification between MI-Anterior and MI-inferior and denoted them as Best Combination or BC-Ant-Inf.

3.3- Classification Technique

Both best combination sets (BC-H-MI and BC-Ant-Inf) of features were used as inputs to a classifier based on Linear Discriminant Analysis (LDA) (20) with the aim of distinguishing (or separating out) MI patients from Healthy subjects and, subsequently, MI-Anterior and MI-inferior. The resulting discriminant function would be the criterion to assign each record to a particular group or class, based on its values of discriminate variables.

As in Figure 1, in this study a cascade classifier is proposed, which, in its first stage, classifies a given subject population in Healthy or MI from a set of parameters called BC-H-MI. Subsequently, the subjects classified as MI (correctly or incorrectly), entered in the second stage to classify them according to the damage heart area, i.e., in MI-Anterior and MI-inferior.

In other words, to validate the LDA classifier, we applied a *leave one out cross validation* (*loo-cv*) method, that is, all selected ECG-VCG features subsets are used for training, while one is saved and left out, using it to validate the discriminant function. Thereafter, the procedure was ran repeatedly until all of the ECG-VCG features subsets were used up. Similar, procedure was applied for the second classification between MI-anterior and MI-inferior.

4-RESULTS

From 3 QRS-loop parameters, 1 QRS-T-loop index, and 6 (XYZ)-ECG features, the study intended to quantify and assess, first, the morphological differences between VCG-ECG records of patients with MI and healthy subjects, and second, the VCG-ECG differences of patients with MI anterior and MI-Inferior. Descriptive analysis results are shown in Figure 3 and Figure 4, respectively, where mean values (M) and standard deviations (SD) are plotted. They were computed for each ECG-VCG record of Healthy and MI Subjects. The statistical significance p-values comparing both populations are also included. In patients with more than one ECG record during the first week after the MI episode, we averaged out the parameter values, so that each corresponded to a single value for each index.

figure 3

figure 4

To evaluate the first stage classification performance, we determined 3 statistical indexes to compare the results predicted by the proposed algorithm against the classification given by the database. These indexes were sensitivity (Sen), specificity (Spe) and accuracy (Acc) and were computed considering a true positive value as patients with MI and a true negative as healthy subjects, correctly classified, respectively. Table 1 shows the results of the *loo*-cv using each parameter and BC-H-MI for the classification between Healthy and MI subjects. The BC-H-MI combination was composed of $\boldsymbol{QRS}_{V}$, $\boldsymbol{QRS}_{PA}$, $\boldsymbol{ST\text{-}T}_{VD}$, $\boldsymbol{T}_{VD}$ and $\boldsymbol{aT}_{X}$.

Table 1

Table 2 a) shows the confusion matrix computed for second stage classification between MI-Anterior and MI-inferior and in b) the *loo-cv* performance indexes using only the BC-Ant-Inf combination. Hence, the BC-Ant-Inf combination was composed of $\boldsymbol{QRS}_{P}$, $\boldsymbol{aQRS}_{X}$, $\boldsymbol{aQRS}_{Y}$, $\boldsymbol{aQRS}_{Z}$, $\boldsymbol{aQRS\text{-}T}_{S}$, $\boldsymbol{aT}_{X}$, $\boldsymbol{aST}_{Y}$ and $\boldsymbol{aST}_{Z}$. It is important to highlight that, in this case, we have 3 classes of subjects: Healthy, ant_MI and inf_MI, using the following equation for computing the performance index (21,22):

$$\boldsymbol{Sen} = \frac{\sum True\ Positive}{\sum Condition\ Positive} \tag{4}$$

$$\boldsymbol{Spe} = \frac{\sum True\ Negative}{\sum Condition\ Negative} \tag{5}$$

$$\boldsymbol{Acc} = \frac{\sum True\ Positive + \sum True\ Negative}{\sum Total\ population} \tag{6}$$

Table 2

5-DISCUSSION AND CONCLUSIONS

In later years, several researchers have proposed different techniques using the same database (PTB) to identifying patients with MI, based on the surface ECG. Among them, the following stand out: Keshtkar *et al*. (8), who proposed the evaluation of the wavelet coefficients set computed over the average ECG signal through neural networks as indexes to detect the MI, and so achieving a Sen = 93%, Spe = 86% and Acc = 89.5%. Bakul *et al*.(7), who have developed a set of features called Relative Frequency Band Coefficient to automatic identification of MI risk, reached a Sen = 85.57%, Spe = 83.97% and Acc = 85.23%. Although all these techniques have their advantages and disadvantages, no one refers to patients, age, gender, days since suffering MI, and other clinical data. As far as we know, however, no report exists regarding how many, or wished-records per patient were used.

The literature, displays reports showing different ways to address the identification of the infarcted area. So, Safdarian *et al.*(10) applied feature extraction from ECG signals and several classifiers for the location of the MI; these authors reached over 76% for accuracy, in test data for localization in four classes (Healthy, Anterior, Inferior, and Posterior). Similarly, Arif *et al*. (9) presented an automatic method for MI localization using K-nearest neighbor, obtaining an accuracy of 98.3% for localization. Even though the techniques proposed by these

researchers have shown very good performance, no reference to patients' age, gender, days since MI, and other clinical data is given.

This work proposes a new technique for the identification of patients with MI and subsequently, estimates the localization of the infarcted area in groups MI-ant and MI-inf. With this aim, we only used the ECG's obtained during the week after MI for each patient and proposed 5 depolarization and 4 repolarization indexes, such as: (a) volume, (b) planar area, (c) perimeter of the QRS loop assessed on 3-D VCG representation ($\boldsymbol{QRS}_{V}$, $\boldsymbol{QRS}_{PA}$ and $\boldsymbol{QRS}_{P}$ respectively); (d) QRS vector difference ($\boldsymbol{QRS}_{VD}$); (e-g) Area under QRS complex, T wave and ST segment in X, Y, Z, leads (***aQRS***, ***aT*** and ***aST***, respectively); (f) ST-T Vector Magnitude Difference ($\boldsymbol{ST\text{-}T}_{VD}$); (h) T-wave Vector Magnitude Difference ($\boldsymbol{T}_{VD}$) The spatial angle between QRS complex and T wave (***aQRS-T***) was also analyzed (see Figure 3 and Figure 4). It can be seen that mean values have a large dispersion because their standard deviations' are often close to the mean. However, the statistical comparison produced significant differences (p-value <0.05) in 12 of the 18 analyzed index (Figure 3), suggesting that they may be used to correctly differentiate between Healthy and MI populations. Similarly, in Figure 4 we can observe that statistical comparison between patients with MI inferior and anterior produced significant differences in 12 of the 18 analyzed indexes (Figure 4).

Table 1 shows that the parameters with greater individual discriminating power between Healthy and MI subject are $\boldsymbol{QRS}_{PA}$ and $\boldsymbol{aT}_{X}$, also when combined with $\boldsymbol{QRS}_{V}$, $\boldsymbol{ST\text{-}T}_{VD}$ and $\boldsymbol{T}_{VD}$, with a Sen = 95.78%, Spe = 94.23% and Acc=95.23%. This demonstrates the excellent performance of the proposed classification technique as compared with other researchers' results (7,8).

In the same way, the cascade classification performance between patients with MI inferior (MI_Inf) and Anterior (MI_Ant) presented in Table 2 a) and b) shows that we could separate out these groups with a Sen = 89.80%, 84,78%, respectively, and Acc = 89,80%. In this classification stage, we used a discriminat function with a combination of $\boldsymbol{QRS}_{P}$, $\boldsymbol{aQRS}_{X}$, $\boldsymbol{aQRS}_{Y}$, $\boldsymbol{aQRS}_{Z}$, $\boldsymbol{aQRS\text{-}T}_{S}$, $\boldsymbol{aT}_{X}$, $\boldsymbol{aST}_{Y}$ and $\boldsymbol{aST}_{Z}$ indexes.

We conclude that the new multivariable MI patient identification and localization technique based on ECG and VCG indexes achieved excellent performance in differentiating populations with MI and healthy subjects. Furthermore, the classification technique estimated the localization of the infarcted area (in two groups MI-ant and MI-inf). It could well become an alternative diagnostic technique in the emergency room. Additionally, it has a low cost, it is non-invasive, and it does not lead to any adverse effect if applied repeatedly.

Acknowledgments

Supported by grants from Consejo Nacional de Investigaciones Científicas y Técnicas (CONICET – PIP538); Consejo de Investigaciones Científicas y de Creación Artística - Universidad Nacional de San Juan (CICITCA-UNSJ – Res. 018/014-CS), and Secretaría de Ciencia, Tecnología e Innovación - Universidad Nacional de San Juan (SECITI-UNSJ – Res. 022/13 CS).

REFERENCES

1. Thygesen K, Alpert JS, Jaffe AS, Simoons ML, Chaitman BR, White HD, et al. Third Universal Definition of Myocardial Infarction. Journal of the American College of Cardiology. 2012;60(16):1581–1598.

2. Manocha AK, Singh M. An overview of ischemia detection techniques. International Journal of Scientific & Engineering Research. 2011;

3. Dilger J, Pietsch-Breitfeld B, Stein W, Overkamp D, Ickrath O, Renn W, et al. Simple computer-assisted diagnosis of acute myocardial infarction in patients with acute thoracic pain. Methods Inf Med. 1992;31:263–267.

4. Correa R, Arini PD, Valentinuzzi ME, Laciar E. Novel set of vectorcardiographic parameters for the identification of ischemic patients. Medical Engineering & Physics. 2013;35(1):16–22.

5. Correa R, Arini PD, Correa L, Valentinuzzi ME, Laciar E. Acute myocardial ischemia monitoring before and during angioplasty by a novel vectorcardiographic parameter set. Journal of electrocardiology. Elsevier; 2013;46(6):635–643.

6. Correa R, Arini PD, Correa LS, Valentinuzzi M, Laciar E. Novel technique for ST-T interval characterization in patients with acute myocardial ischemia. Computers in biology and medicine. Elsevier; 2014;50:49–55.

7. Bakul G, Tiwary U. Automated risk identification of myocardial infarction using relative frequency band coefficient (RFBC) features from ECG. The open biomedical engineering journal. Bentham Science Publishers; 2010;4:217.

8. Keshtkar A, Seyedarabi H, Sheikhzadeh P, others. discriminant analysis between myocardial infarction patients and healthy subjects using Wavelet Transformed signal averaged electrocardiogram and probabilistic neural network. Journal of Medical Signals and Sensors. 2013;3(4).

9. Arif M, Malagore IA, Afsar FA. Detection and localization of myocardial infarction using K-nearest neighbor classifier. Journal of medical systems. Springer; 2012;36(1):279–289.

10. Safdarian N, Dabanloo NJ, Attarodi G. A New Pattern Recognition Method for Detection and Localization of Myocardial Infarction Using T-Wave Integral and Total Integral as Extracted Features from One Cycle of ECG Signal. Journal of Biomedical Science and Engineering. Scientific Research Publishing; 2014.

11. Bousseljot R, Kreiseler D, Schnabel A. Nutzung der EKG-Signal daten bank CARDIODAT der PTB über das Internet. Biomedizinische Technik, Band 40, Ergänzungsband. 1995;1:317.

12. Goldberger AL, Amaral LAN, Glass L, Hausdorff JM, Ivanov PC, Mark RG, et al. PhysioBank, PhysioToolkit, and PhysioNet: Components of a New Research Resource for Complex Physiologic Signals. Circulation. 2000;101(23):e215–e220.

13. Gutierrez A, Lara M, Hernandez PR. A QRS Detector Based on Haar Wavelet, Evaluation with MIT–BIH Arrhythmia and European ST–T Databases. Computacion y Sistemas. scielomx; 2005;8:293–302.

14. Martinez JP, Almeida R, Olmos S, Rocha AP, Laguna P. A wavelet-based ECG delineator: evaluation on standard databases. Biomedical Engineering, IEEE Transactions on. 2004 Apr;51(4):570–581.

15. Laciar E, Jane R, Brooks DH. Improved alignment method for noisy high-resolution ECG and Holter records using multiscale cross-correlation. Biomedical Engineering, IEEE Transactions on. 2003 Mar;50(3):344–353.

16. Kardys I, Kors JA, Meer IM van der, Hofman A, Kuip DA. van der, Witteman JCM. Spatial QRS-T angle predicts cardiac death in a general population. European Heart Journal. The Oxford University Press; 2003;24(14):1357–1364.

17. Rubulis A, Bergfeldt L, Rydén L, Jensen J. Prediction of cardiovascular death and myocardial infarction by the QRS-T angle and T vector loop morphology after angioplasty in stable angina pectoris: an 8-year follow-up. Journal of electrocardiology. Elsevier; 2010;43(4):310–317.

18. Dellborg M, Malmberg K, Ryden L, Svensson A, Swedberg K. Dynamic on-line vectorcardiography improves and simplifies in-hospital ischemia monitoring of patients with unstable angina. Journal of the American College of Cardiology. 1995;26(6):1501–1507.

19. Hall P, Hallén B, Selander H. Linear discriminatory analysis: a patient classifying method for research and production control. Methods Inf Med. 1971;(Vol. 10): Issue 2:96–102.

20. Flores JG, Jiménez EG, Gómez GR. Análisis discriminante. La Muralla; 2001.

21. Powers DM. Evaluation: From Precision, Recall and F-Factor to ROC, Informedness, Markedness & Correaltion. Adelaide: School of Informatics and Engineering, Flinders University of South Australia; 2007.

22. Sokolova M, Lapalme G. A systematic analysis of performance measures for classification tasks. Information Processing & Management. 2009;45(4):427–437.

Figure 1 -

General block diagram of the proposed technique.

Figure 2 -

VCG and ECG parameters computation.

Figure 3 –

Mean values (M) and standard deviations (SD) and statistical significance (p-value) of each parameter for Healthy vs MI populations.

Figure 4 -

Mean values, standard deviations and statistical significance (p-value) of each parameter for MI-Ant vs MI-Inf population.

TABLE

Table 1 –

Classification outcomes for each computed index and for the BC-H-MI.

Table 2 –

a) Confusion Matrix and b) Classification outcomes for the BC-Ant-Inf.

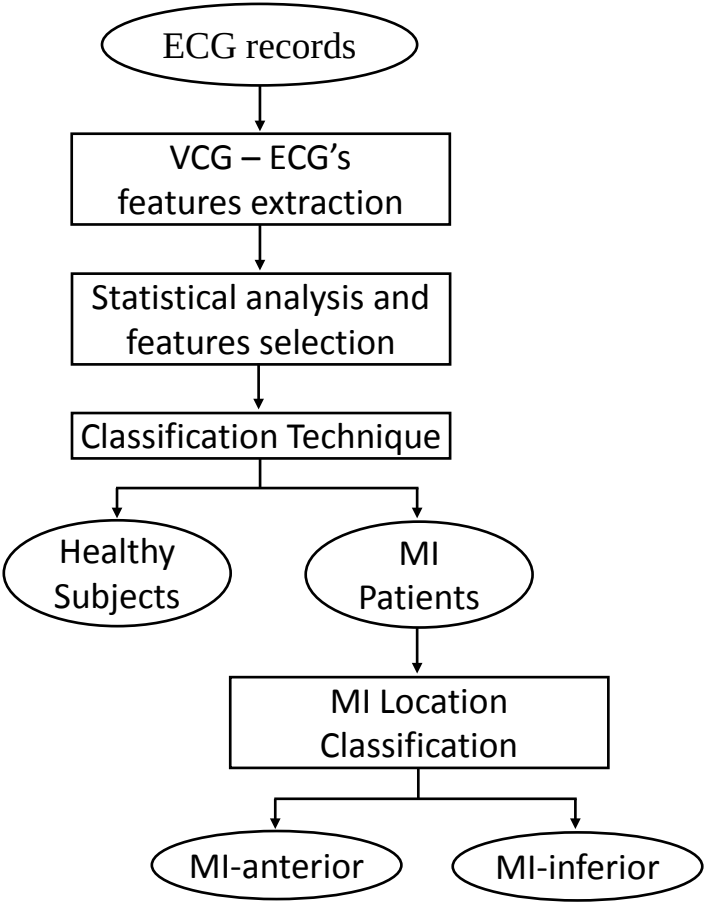
ECG records
VCG – ECG's features extraction
Statistical analysis and features selection
Classification Technique
Healthy Subjects
MI Patients
MI Location Classification
MI-anterior
MI-inferior

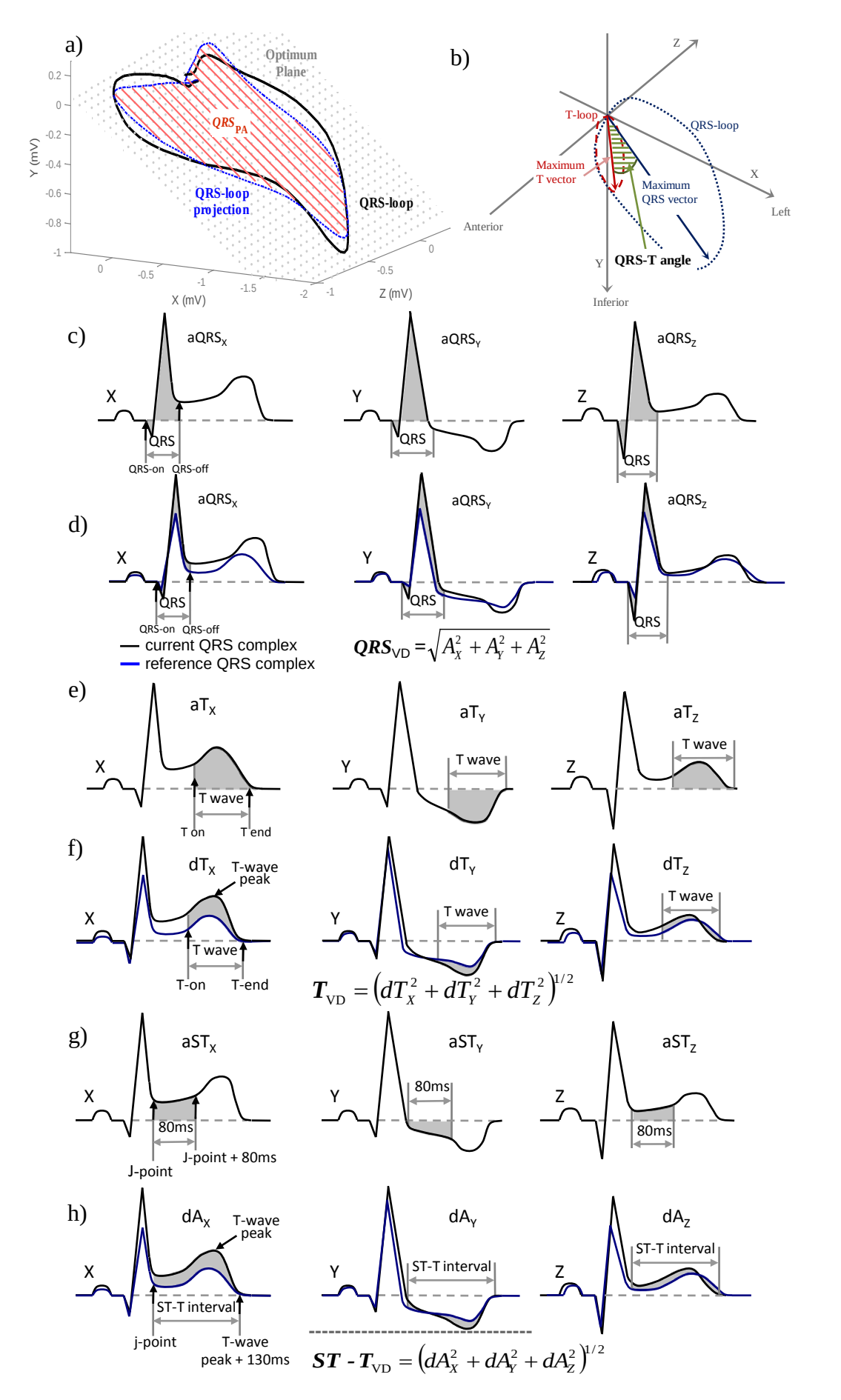
a)
Optimum Plane
QRS_PA
QRS-loop projection
QRS-loop
Y (mV)
X (mV)
Z (mV)
b)
Z
T-loop
QRS-loop
Maximum T vector
Maximum QRS vector
X
Left
Anterior
Y
QRS-T angle
Inferior
c)
aQRS_X
aQRS_Y
aQRS_Z
X
Y
Z
QRS
QRS-on
QRS-off
d)
current QRS complex
reference QRS complex
QRS_VD = √(A_X² + A_Y² + A_Z²)
e)
aT_X
aT_Y
aT_Z
T wave
T on
T end
f)
dT_X
dT_Y
dT_Z
T-wave peak
T-on
T-end
T_VD = (dT_X² + dT_Y² + dT_Z²)^1/2
g)
aST_X
aST_Y
aST_Z
80ms
J-point
J-point + 80ms
h)
dA_X
dA_Y
dA_Z
ST-T interval
j-point
T-wave peak + 130ms
ST - T_VD = (dA_X² + dA_Y² + dA_Z²)^1/2

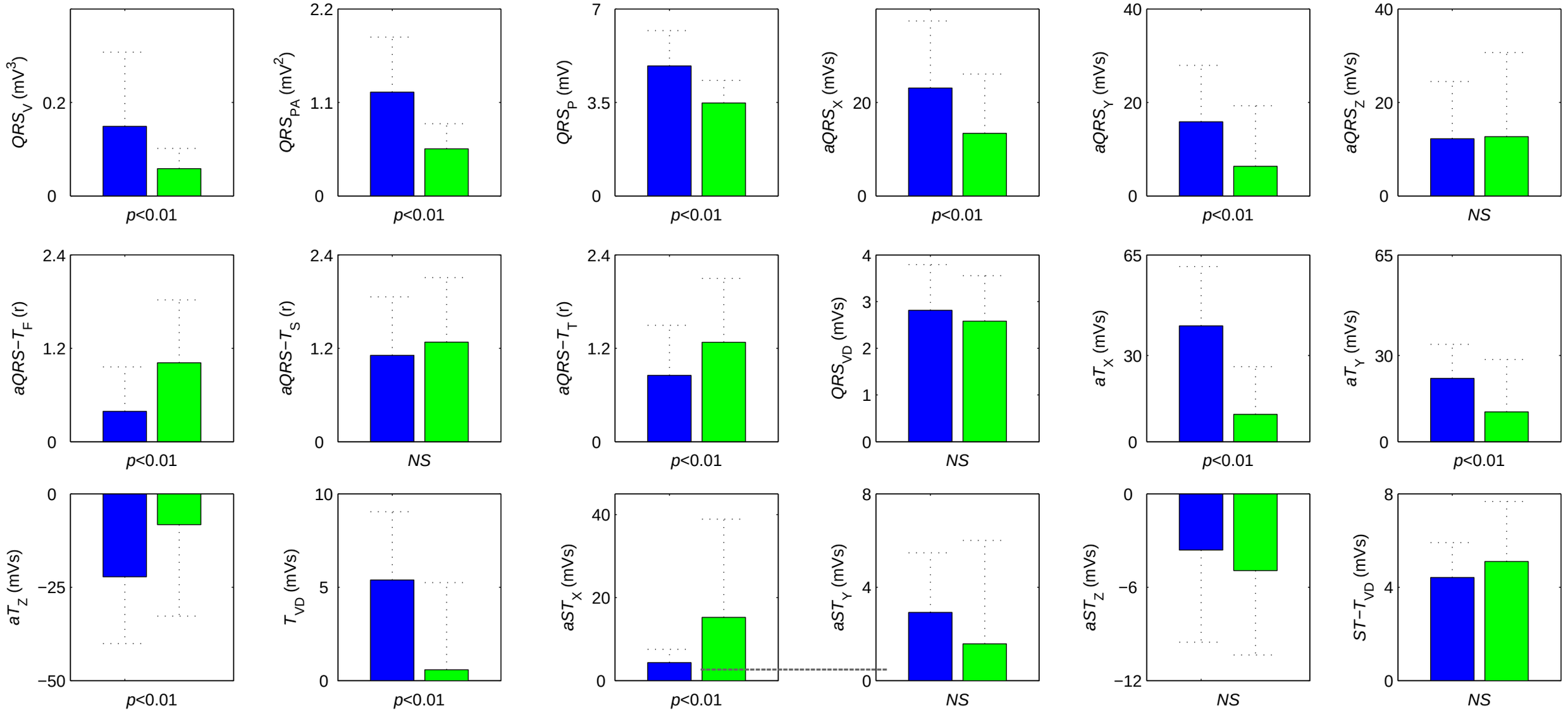
QRS_V (mV^3)
0.2
0
p<0.01
QRS_{PA} (mV^2)
2.2
1.1
0
p<0.01
QRS_P (mV)
7
3.5
0
p<0.01
$aQRS_X$ (mVs)
20
0
p<0.01
$aQRS_Y$ (mVs)
40
20
0
p<0.01
$aQRS_Z$ (mVs)
40
20
0
NS
$aQRS{-}T_F$ (r)
2.4
1.2
0
p<0.01
$aQRS{-}T_S$ (r)
2.4
1.2
0
NS
$aQRS{-}T_T$ (r)
2.4
1.2
0
p<0.01
QRS_{VD} (mVs)
4
3
2
1
0
NS
aT_X (mVs)
65
30
0
p<0.01
aT_Y (mVs)
65
30
0
p<0.01
aT_Z (mVs)
0
−25
−50
p<0.01
T_{VD} (mVs)
10
5
0
p<0.01
aST_X (mVs)
40
20
0
p<0.01
aST_Y (mVs)
8
4
0
NS
aST_Z (mVs)
0
−6
−12
NS
$ST{-}T_{VD}$ (mVs)
8
4
0
NS

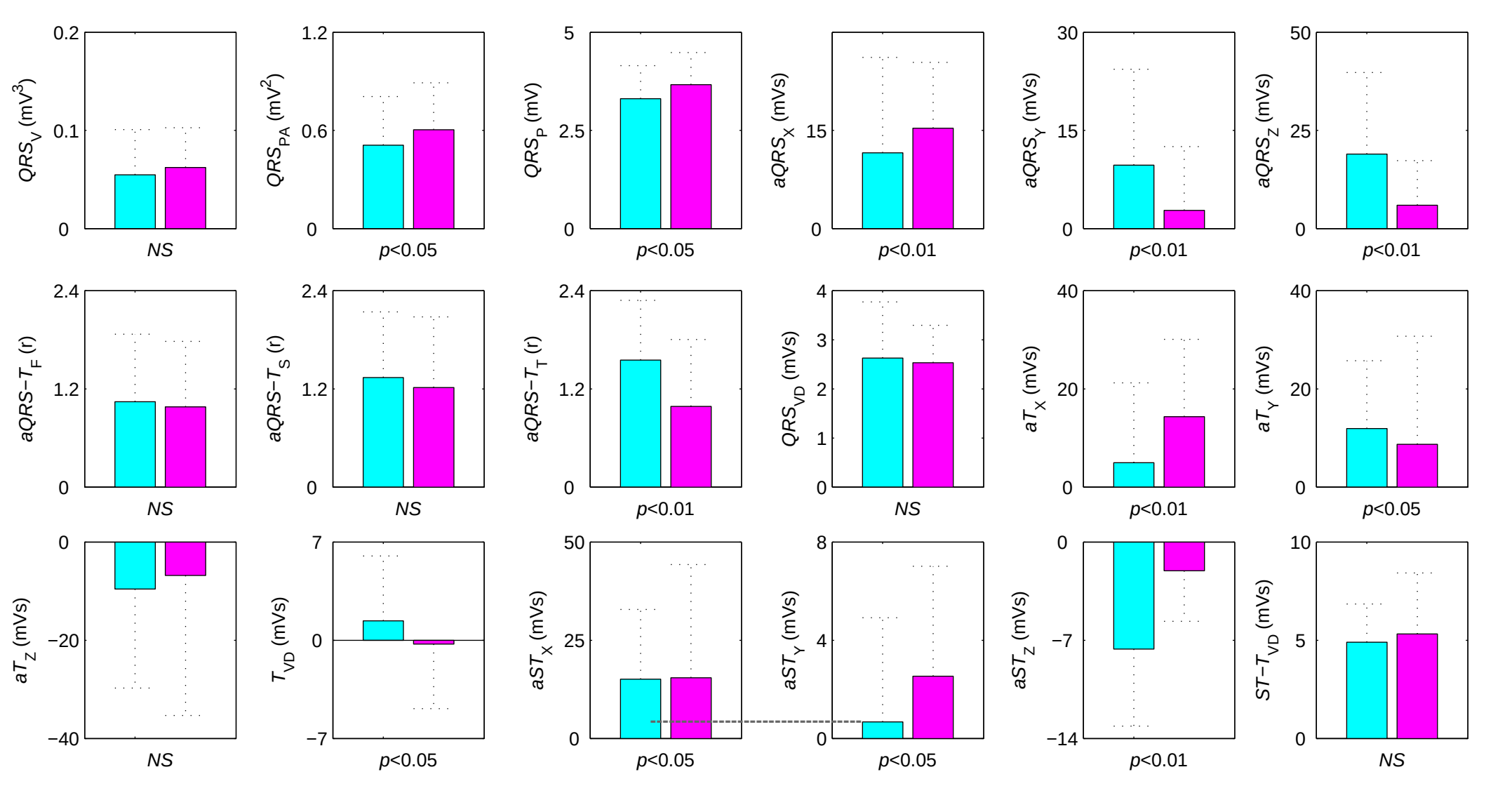
QRS_V (mV^3)
0.2
0.1
0
NS
QRS_{PA} (mV^2)
1.2
0.6
0
p<0.05
QRS_P (mV)
5
2.5
0
p<0.05
$aQRS_X$ (mVs)
30
15
0
p<0.01
$aQRS_Y$ (mVs)
30
15
0
p<0.01
$aQRS_Z$ (mVs)
50
25
0
p<0.01
$aQRS{-}T_F$ (r)
2.4
1.2
0
NS
$aQRS{-}T_S$ (r)
2.4
1.2
0
NS
$aQRS{-}T_T$ (r)
2.4
1.2
0
p<0.01
QRS_{VD} (mVs)
4
3
2
1
0
NS
aT_X (mVs)
40
20
0
p<0.01
aT_Y (mVs)
40
20
0
p<0.05
aT_Z (mVs)
0
−20
−40
NS
T_{VD} (mVs)
7
0
−7
p<0.05
aST_X (mVs)
50
25
0
p<0.05
aST_Y (mVs)
8
4
0
p<0.05
aST_Z (mVs)
0
−7
−14
p<0.01
$ST{-}T_{VD}$ (mVs)
10
5
0
NS

	QRS_V	QRS_{PA}	QRS_P	$aQRS_X$	$aQRS_Y$	$aQRS_Z$	$aQRS\text{-}T_F$	$aQRS\text{-}T_S$	$aQRS\text{-}T_T$	QRS_{VD}
Sen (%)	91.58	92.63	81.05	76.84	70.53	98.95	60.00	60.00	60.00	69.47
Spe (%)	48.08	67.31	69.23	42.31	55.77	0.00	84.62	42.31	69.23	36.54
Acc (%)	76.19	83.67	76.87	64.63	65.31	63.95	68.71	53.74	63.27	57.82

	aT_X	aT_Y	aT_Z	T_{VD}	aST_X	aST_Y	aST_Z	$ST\text{-}T_{VD}$	**BC-H-MI**
Sen (%)	86.32	72.63	70.53	82.11	50.53	68.42	65.26	61.05	**95.79**
Spe (%)	75.00	57.69	55.77	67.31	90.38	46.15	42.31	53.85	**94.23**
Acc (%)	82.31	67.35	65.31	76.87	64.63	60.54	57.14	58.50	**95.23**

a)

		Predicted			Total
		Healthy	Ant_MI	Inf_MI	
Real	Healthy	49	0	3	52
	Ant_MI	2	44	3	49
	Inf_MI	2	5	39	46

b)

	Healthy	Ant_MI	Inf_MI
Sen (%)	94.2	89.8	84.8
Spe (%)	87.4	89.8	92.1
Acc (%)	89.8	89.8	89.8